

# Short-term Accumulations Forecasting Using License Recognition Data

Lei Jin, Binglei Xie

**Abstract**—The emerging accumulation-based emerging perimeter control strategy in the context of Macroscopic Fundamental Diagrams (MFD) need to predict accumulations dynamically. The objective of this study is to present short-term accumulations forecasting problem. Forecasting models and its inputs vectors of traffic accumulations should be studied firstly. To avoid the drawback of fuzzy descriptions for link traffic states derived by traffic arrivals, this study newly proposes a method to monitor the dynamics of link accumulations in the context of MFDs. This method yields a full description of the MFD by relating the number of circulating vehicles (accumulations) to network flow (arrivals). The precise traffic data are extracted from discrete records of automatic license plate recognition database. In addition, this paper studies possible applications and accuracy levels of four machine learning models for short-term accumulation forecasting: back-propagation neural network (BPNN), wavelet neural network (WNN), radial basis function neural networks (RBFNN) and support vector regression (SVR). WNN and BPNN models are found to be adaptive and have accuracy levels only a sixth that of RBFNN and SVR models.

**Index Terms**—urban traffic system dynamics; traffic state estimation; short-term accumulations forecasting; automatic license plate recognition data; machine learning

## I. INTRODUCTION

Overload vehicles in urban road sections can lead to congestion, even gridlock in network-wide. The dynamic characteristics of discrete vehicles should be investigated to deal with intelligent traffic management technologies [1,2]. Modeling and forecasting vehicular traffic flows have been proposed for decades [3,4]. For example, most signal control strategies start with predictions of traffic arrivals, which are highly rely on the dynamics of arrivals at signalized intersections [5,6]. However, capturing the discrete traffic arrivals dynamics cannot give transportation engineers the whole picture of network congestion. Local control strategies relying on short-term traffic arrivals forecasting fail to care for the distribution of network traffic density. Besides, applications of control approaches based on microscopic modeling of traffic flow are confronted with some obstacles, such as huge complex of control strategies and unpredictability of driver navigations. Instead of microscopic modeling of traffic arrivals at disaggregate level, macroscopic modeling of traffic flows at aggregate level was

proposed for macroscopic monitoring and control in urban road network, which could capture the aggregation characteristics of traffic flow [1,7,8].

For a further attempt in this direction, the purpose of this paper is to design a methodology to model and forecast accumulation of vehicles in freeways that play the role of transferring flows. This problem is a complicated one as the nonlinear accumulations in parts of network is caused by disproportionate relationship between vehicle arrivals and departures. Accurate modeling of nonlinear accumulation of vehicles as a continuous phenomenon has to take disproportionate relationship into consideration. This paper develops a method for modeling the nonlinear accumulations using automatic license plate recognition data (ALPRD). The suggested modeling method can provide accumulations as constant input vectors of short-term forecasting models. This paper also presents a short-term accumulations forecasting problem based on machine learning methods with a new insights in traffic accumulation prediction. After this construction, the proposed solution framework would be regarded as a bridge between microscopic traffic flow dynamics and macroscopic system dynamics for traffic monitoring and management.

The paper is organized as follows. Section 2 introduces the background and presents short-term accumulations forecasting problem. Section 3 shows four basic models for short-term freeway accumulations forecasting. Section 4 presents a data-driven approach for numeric inputs by modeling freeway accumulations. Section 5 discusses the experimental results. Section 6 concludes the paper and discusses the future research.

## II. SHORT-TERM ACCUMULATIONS FORECASTING PROBLEM

### A. Problem Formulation

With the disproportionate number of input and output of vehicles, accumulations have made a significant contribution to saturated and over-saturated states of urban road networks. If accumulations exceeds the capacity of subnetworks, the arrivals of vehicles would decrease in the flow and even lead to gridlock in subnetworks. In order to propose perimeter control schemes to prevent saturated and over-saturated states of subnetworks, the first thing transportation engineers need to do is capture dynamics of accumulation in road sections [9]. Modeling and forecasting of aggregation characteristics of traffic flow in arterial freeways can be utilized to replace tasks of monitor and predict traffic flow in microscopic perspective [10]. The dynamic characteristics of traffic flow are derived from traffic arrivals, accumulations and

Lei Jin, Ph.D Student, School of Architecture and Urban Planning, Harbin Institute of Technology, Shenzhen, Guangdong, P.R. China

Binglei Xie, Professor, School of Architecture and Urban Planning, Harbin Institute of Technology, Shenzhen, Guangdong, P.R. China

departures. These can be monitored by strong detection components regardless of travel patterns and dynamic origin-destination (O-D) conundrums in the context of Macroscopic Fundamental Diagrams (MFD) [11].

Modeling of network dynamics with an aggregation framework was proposed in [1], and computed by empirical loop data and taxi GPS data [2,12]. The relationship between network vehicle density (related to accumulation) and network space-mean flow have been investigated as MFD [2]. These papers showed that accumulations both in subnetworks and links are not sensitive to different demands. Furthermore, a generalized macroscopic fundamental diagram (GMFD) for urban freeways was developed to relate accumulations to spread of density, which showed inhomogeneous distribution of accumulations in network [13,14]. The dynamic pattern of accumulation can be used to estimate traffic state of subnetworks.

The MFD-based control strategies need real-time data which can be monitored and obtained by traffic control system, i.e., the dynamic characterization of MFD which is consist with mathematical needs of linear control system. Actually, MFD-based linear control systems are often based on distinct variables of the MFD and direct sequential method. The dynamic processes of MFD can be decomposed into nonlinear time-varying patterns of network average flow and network average density.

### B. Problem Definition

The input-output systems of transportation networks can be considered as sets of inter-connected reservoirs (grids that decomposed from urban area). Dynamic characteristics of traffic flow can be used to capture internal flow and transboundary flow of inter-connected reservoirs. In particular dynamics characteristics of accumulations in subnetworks can be used to improve mobility in network-wide. For multi-reservoirs systems, accumulations could be dynamically managed by restricting the transfer of flows between inter-connected reservoirs with accumulation-based (AB) strategy for urban areas [1,15]. Freeways in urban road network can be regarded as the major pipelines that transfer flows between inter-connected reservoirs. Similar to major pipeline congestion for reservoir system, congested freeway accumulation can be used to express main aggregate characteristics of subnetwork congestion. If we can monitor characteristics of traffic congestion in reservoirs, strategies that based on short-term forecasting of the macroscopic system dynamics could be used to complete optimal perimeter control.

Time-varying accumulations in sections can be regarded as predictable variable with time series data [2,11]. Accumulations may vary in a dynamic pattern over a regular interval, which mainly caused by the disproportionate relationship of arrivals and departures. Once the optimal perimeter of accumulations in reservoirs is determined, accumulations could be regulated by restricting the transfer of flows between abutting and separated reservoirs. The most effective strategy is to keep transfer efficiency of freeways as close to optimal state, which means that keep accumulations as close to optimal value. A development effort is also needed to predict accumulations dynamically that would support

optimal perimeter control schemes for improving accessibility in subnetworks [1,2].

Feasibility study of accumulations prediction problem have been argued in [1] and [11]. The two references suggested that forecast-based approaches of accumulations prediction could be effective if complemented with real-time monitoring of the state variables. With accumulations as a state perimeter, a prediction model for capture the evolution of accumulations was proposed in [11]. The model operates by initial accumulations and future values of perimeter control inputs with loop detector data. It would be difficult to observe outflows by loop detectors, so that the mentioned studies are based on the postulate that trip completion rate is proportional to production [2,11]. However, the outflows of a subnetwork or section are actually independent of its inputs. The postulates is a marked difference from the macroscopic modeling aggregation hypothesis originally presented in [1]. The statistics information based on loop detector data can only be regard as fuzzy accounting for road traffic states. To all appearance, the availability of data limited the study on dynamics of accumulations and affected the development of optimal perimeter control schemes based on short-term macroscopic traffic flow forecasting. The further scrutiny should include field experiments considering disproportionate relationship between inputs and outputs.

## III. MODELS

In practice, short-term accumulations forecasting is useful for a range of purposes, such as real-time monitoring and perimeter control. Accumulations is a critical element which could provide the basis of reliable tools that anticipate results of traffic management policies. For example, policies based on short-term forecasting of macroscopic system dynamics could be effective if complemented with real-time monitoring of the state variables [1].

Short-term forecasting models can be used to capture urban link accumulations dynamically. Short-term traffic flow forecasting is considered as an excellent field for developing and testing complex prediction algorithms based on current and past traffic information, which can be used to model traffic characteristics such as volume, density and speed, or travel times, and produce anticipated traffic conditions [16,17]. Some empirical computational intelligence-based approaches like neural networks, fuzzy and evolutionary algorithm are used in short-term traffic flow prediction problems. In this section, four data-driven models are presented to predict short-term accumulations dynamically, including back-propagation neural network (BPNN), wavelet neural network (WNN), radial basis function neural networks (RBFNN) and support vector regression (SVR).

### A. Back-propagation Neural Network

Back-propagation neural network (BPNN) has a powerful ability of non-linear interpolation by using a supervised learning method and feed-forward architecture, which can be used for traffic flow forecasting [18] and risk prediction [19]. BPNN is trained by training algorithm in order to obtain the ability of memory and prediction. The output of hidden layer

is calculated with the following formula Eq. (1):

$$H(j) = f\left(\sum_{i=1}^n w_{ij}x_i - a_j\right) \quad j = 1, 2, \dots, l \quad (1)$$

where  $X = x_1, x_2, \dots, x_k$  is the vector of inputs,  $H(j)$  is the output of  $j$ -th hidden node,  $w_{ij}$  is the weight for the connections between the input layer  $i$  and hidden layer  $j$ .  $f$  is the active function of hidden layer neurons as Eq. (2):

$$f(x) = (1 + \exp(-x))^{-1} \quad (2)$$

The formula of output layer is as Eq. (3):

$$p(k) = \sum_{j=1}^m w_{jk}H(j) - \xi_k \quad k = 1, 2, \dots, m \quad (3)$$

where  $w_{jk}$  is the weight for the connections between the hidden layer  $j$  and output layer  $k$ .

BP neural networks are trained by a supervised learning algorithm. The BP network learning process includes two stages: the first stage is to input the known learning samples array and setting up the network structure, the second stage is to modify the weights and thresholds of the network in an iterative way so that the trained network fits the training samples well. The whole training of the BPNN is completed until the overall error between calculated and desired output is less than error criteria, or the number of iteration reaches the fixed value.

### B. Wavelet Neural Network

Wavelet neural network are based on the BPNN network and a wavelet transform has properties that are superior to a conventional Fourier transform, which can be used for traffic flow forecasting [20] and traffic incidents detection [21]. The WNN consists of three layers: input layer, hidden layer and output layer. All nodes in each layer are connected to the nodes in the next layer.

WNN is implemented with the wavelet function and training algorithm. The output of hidden layer is calculated with the following formula Eq. (4):

$$H(j) = f_j\left(\left(\sum_{i=1}^k w_{ij}x_i - b_j\right)/a_j\right) \quad j = 1, 2, \dots, l \quad (4)$$

where  $H(j)$  is the output of the number  $j$ -th of hidden nodes,  $w_{ij}$  is the weight for the connections between the input layer  $i$  and hidden layer  $j$ .  $H(j)$  is taken as a Morlet mother wavelet with the following formula Eq. (5):

$$f(x) = \cos(1.75x) \exp\left(-\frac{x^2}{2}\right) \quad (5)$$

The formula of output layer is as Eq. (6):

$$p(k) = \sum_{j=1}^l w_{jk}H(j) \quad k = 1, 2, \dots, m \quad (6)$$

where  $w_{jk}$  is the weight for the connections between the hidden and output layer. The whole training of the WNN is completed until error satisfies the given error criteria, otherwise, return to predict the output again.

### C. Radial Basis Function Neural Network

Radial Basis Function Neural Network (RBFNN) is a three-layer feed-forward neural network with a supervised algorithm and has been employed for classification and interpolation regression [23], which can be used for traffic flow forecasting [23-25] and traffic incidents detection [26]. The RBFNN is approximate continuous function with a prospected accuracy, which includes three layers: an input layer, a nonlinear hidden layer (radial basis layer) and a linear output layer. The real output in output layer is calculated using Eq. (7):

$$p(k) = \sum_{j=1}^k w_{js} \varphi\left(\|a(k) - C_j\| / \sigma_j\right) \quad \text{for } 1 \leq s \leq l \quad (7)$$

where  $X$  is input vector of the network,  $y_s$  is the  $s$ -th network output,  $a(k)$  represents input patterns extracted from  $X$ ,  $w_{js}$  is the weight of the link between  $j$ -th hidden neuron and  $s$ -th output neuron,  $C_j$  is the center of the  $j$ -th RBF unit in the hidden layer, and  $\sigma_j$  is the width of the  $j$ -th unit in the hidden layer.  $\varphi$  denotes a basis function which is most generally instantiated by a Gauss function as Eq. (8):

$$\varphi_j(r) = \exp\left(-\|a(k) - C_j\|^2 / 2\sigma_j^2\right) \quad j = 1, 2, 3, \dots, p \quad (8)$$

where  $r$  is the variable of radial basis function  $\varphi$ .

### D. Support Vector Regression

Support Vector Regression (SVR) is employed to tackle with problems of function approximation and regression estimation [27], which can be used for traffic flow forecasting [28] and traffic incidents detection [29]. In general, the approximating function in SVR takes the following linear form Eq. (9):

$$p(x) = w\varphi(x) + b \quad (9)$$

where  $x$  is input features,  $w$  is weight vector,  $\varphi$  is the high-dimensional feature space, which is non-linearly mapped from the input space and  $b$  denotes the bias.

The following convex optimization problem can be formulated as Eq. (10):

$$\min \frac{1}{2} \|w\|^2 + C \sum_{i=1}^n (\xi_i + \xi_i^*) \quad (10)$$

where  $\xi_i$  and  $\xi_i^*$  are two slack variables to cope with infeasible constraint of the optimization problem and represent the upper and lower boundaries of insensitive zone.

Then Lagrange multipliers are used to solve a dual optimization problem in support vector machine. Finally, by exploiting the optimization problem in terms of kernel function takes the following formula Eq. (11):

$$f(x) = \sum_{i=1}^n (a_i - a_i^*) \exp(-\gamma \|x_i - x_j\|)^2 + b \quad (11)$$

where  $a_i$  and  $a_i^*$  are Lagrange multipliers.

IV. A DATA-DRIVEN APPROACH FOR NUMERIC INPUTS OF MODELS

Numeric input vector of short-term accumulations forecasting models consisted of link accumulations in specific time intervals. This section presents an improved aggregation method to estimate accumulations using automatic license plate recognition data. Automatic license plate recognition data is collected by the automatic license plate recognition system embedded in urban road transport system continuously. Comparing the aggregation methods based on loop detector data and automatic license plate recognition data mentioned above, the latter method could be summarized as an estimating method which is more closed to the reality of link traffic states.

A. Field Automatic License Plate Recognition Data Collection

In order to derive the basic aggregation parameters of traffic state, this study uses automatic license plate recognition data to count and calculate arrivals, accumulations and departures of vehicles. The database are recorded by road cameras fixed on road gantries along roads. The items of travel status recorded by the road cameras are independent. One item contains corresponding vehicles' plate number, vehicle type, velocity, and recording time. Compared to loop detector data, the automatic license plate recognition data can be used to capture characteristics when vehicles driving in sections. As shown in Figure 1, license information and dynamics characteristics of every vehicle can be recorded by two adjacent cameras of the Automatic License Plate Recognition System.

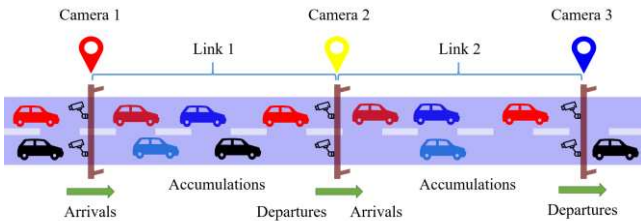


Figure 1: Schematic picture about the dynamics of accumulations.

The database utilized in this research was collected by automatic license plate recognition system from January 12nd, 2015 to January 16th, 2015, which is recorded from eastbound vehicles by road cameras fixed on North Ring Road in Shenzhen, China. One section between the North Ring Xinzhou overpass and Mudhill Redridge overpass with length 6.4 km is considered in this study. The study area faces risk of congestion during rush hour of weekdays. Meanwhile, in order to match needs of control applications, schemes would be much more significative and effective during the time windows of rush hour. In this study, morning rush hour (from 7: 05 to 9: 25) and evening rush hour (from 17: 05 to 19: 25) are selected as time windows. Data are grouped into 5 minute intervals which contains one traffic signal cycle at least.

B. Data-driven Approach for Accumulation Estimation

The purpose of this section is to develop a method to derive link accumulation of road network exactly. The best-known

method of estimating link accumulation is proposed in [1]. A refined MFD is reproducible and relates the number of circulating vehicles (or accumulation) to the network's average speed (or flow). Thus, measuring link accumulation is pivotal to advancing the field of MFD estimation and application. Cameras record camera ID, vehicle's license number, vehicle type, velocity, and recognition time. Traffic flow variables can be calculated using arrival and departure information.

Link accumulation can be theoretically estimated by deviations of upstream arrivals and downstream departures.  $n_i(t)$  is defined as the number of vehicles traveling on link  $i$  at time  $t$ .  $A_i(t)$  and  $L_i(t)$  are defined as the cumulative number of vehicles have arrived and left link  $i$  at time  $t$ , respectively. The urban link accumulation at time  $t$  is derived by following formula  $n_i(t) = A_i(t) - D_i(t)$ . Link accumulation in any time interval  $[t, t + \Delta t]$  is derived by an aggregation formula  $n_i(t, t + \Delta t) = \int_t^{t+\Delta t} n_i(t) dt$ .

In addition, it is important that computing the functions with appropriate database. The loop detector data only provide local snapshots of traffic states that are used as proxies for link traffic states (Leclercq et al., 2014). Therefore, the accurate accumulations should be analyzed and computed by considering effective computational method for link traffic states.

In the following, a method is developed to count the freeway accumulations of vehicles in an independent interval based on automatic license plate recognition dataset. Let  $V^l$  be a set of arrived vehicles on link  $l$ .  $V_i^l(t, t + \Delta t)$  represents entry number  $i$  of vehicles arriving on link  $l$  in time interval  $[t, t + \Delta t]$ . Define  $[nt, nt + \Delta t]$  as  $n$ -th time interval. Let  $U_n$  be sets of time intervals, that is  $U_n = \{[nt, nt + \Delta t] | n \in N, n \neq 0\}$ . Meanwhile, define  $T_{arrived}(V_i^l(t, t + \Delta t))$  as the time that vehicle  $V_i^l(t, t + \Delta t)$  entering link  $l$  in the moment. Define  $T_{left}(V_i^l(t, t + \Delta t))$  as the time that vehicle  $V_i^l(t, t + \Delta t)$  exiting link  $l$  in the moment. By definition,  $T_{arrived}(V_i^l(t, t + \Delta t)) \in [t, t + \Delta t]$ , and  $T_{left}(V_i^l(t, t + \Delta t))$  may belong to  $[t, t + \Delta t]$  or not belong to  $[t, t + \Delta t]$ .

If the moment of vehicle  $V_i^l(t, t + \Delta t)$  entering link  $l$  satisfy the following condition  $T_{arrived}(V_i^l(nt, nt + \Delta t)) \in [nt, nt + \Delta t]$ , and the moment of vehicle  $V_i^l(t, t + \Delta t)$  exiting link  $l$  satisfy the following condition  $T_{left}(V_i^l(nt, nt + \Delta t)) \notin [nt, nt + \Delta t]$ , it is reasonable to assume that the vehicle  $V_i^l(nt, nt + \Delta t)$  is traveling on link  $l$  in the time interval  $[nt, nt + \Delta t]$ , the

relation can be described as Eq. (12):

$$S = \{(T_{arrived}, T_{left}) | T_{arrived}(V_i^l(nt, nt + \Delta t)) \in U_n, T_{left}(V_i^l(nt, nt + \Delta t)) \notin U_n\} \quad (12)$$

For a finite set  $S$ , the unique natural number is called the cardinal number of  $S$ , abbreviated  $card(S)$ . Obviously, the elements  $(T_{arrived}, T_{left})$  of set  $S$  are all independent time pairs. The cardinality of the finite set  $S$  is a natural number, that is the number of time pairs  $(T_{arrived}, T_{left})$  in the set  $S$ .

Denote  $LA^l(nt, nt + \Delta t)$  as the total number of vehicles are traveling on link  $l$  in the time interval  $[nt, nt + \Delta t]$ , which is equivalent to the cardinality of set  $S$ . That is accumulations in time interval  $[nt, nt + \Delta t]$  can be derived exactly as Eq. (13):

$$LA^l(nt, nt + \Delta t) = card(S) = |S| \quad (13)$$

The traffic flow parameters could be calculated by automatic license plate recognition data. Additionally, once the time pairs  $(T_{arrived}, T_{left})$  of vehicles were determined, the travel time and travel speed could also be determined. Therefore, the aggregation traffic flow parameters could be used to estimate link traffic states.

## V. EXPERIMENTS

### A. Performance Measurements

The automatic plate recognition data collected from a freeway in Shenzhen is used to express nonlinear interaction and to compare the predicting performance among proposed models. All experiments on short-term accumulations forecasting are calculated by Matlab R2014a on a laptop with a dual-core 2.50GHz CPU and a 2 GB RAM.

To compare the prediction performance of the four models, the following four error measurements are used to describe the error and non-linear interaction between the actual value  $a(k)$  and the predicted value  $p(k)$ , namely, the mean absolute error (MAE), the mean relative error (MRE), the mean squared error (MSE) and the root mean squared error (RMSE).

The equation of MAE is calculated using Eq. (14):

$$MAE = (\sum_{k=1}^n |p(k) - a(k)|) / n \quad (14)$$

The equation of MRE is calculated using Eq. (15):

$$MRE = (\sum_{k=1}^n | \frac{p(k) - a(k)}{a(k)} |) / n \quad (15)$$

The equation of MSE is calculated using Eq. (16):

$$MSE = (\sum_{k=1}^n |p(k) - a(k)|^2) / n \quad (16)$$

The equation of RMSE is calculated using Eq. (17):

$$RMSE = ((\sum_{k=1}^n |p(k) - a(k)|^2) / n)^{1/2} \quad (17)$$

### B. Application of BPNN

In particular, prediction models are information-processing systems that have specific performance characteristics with numerous simple processing elements called neurons or nodes, which can be applied in non-linear modeling fields. Meanwhile, it is imperative that prediction models should be compared in parameter selection and results. In order to make the models perform well, key parameters of each model are compared in the following model calibrating process by using the same non-linear data series of accumulations.

Single hidden layer architecture is used in the BPNN model. A comparison of different number of neurons in the hidden layer are conducted to determine the optimal BPNN architecture. Figure 2(a) shows the RMSE and MRE for each prediction model with respect to the variations of key parameters. As shown in Figure 2(b), for BPNN, when the number of neurons in the hidden layer is around 15, the performance of model is most stable and accurate.

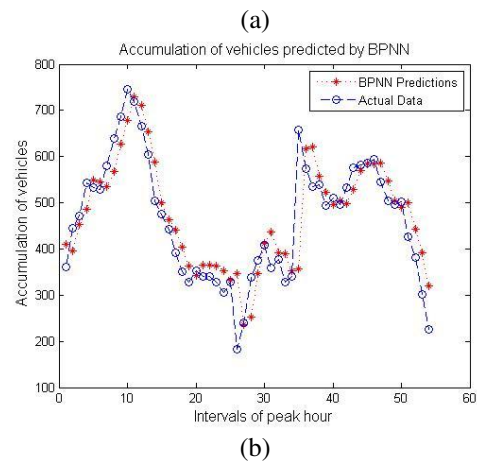
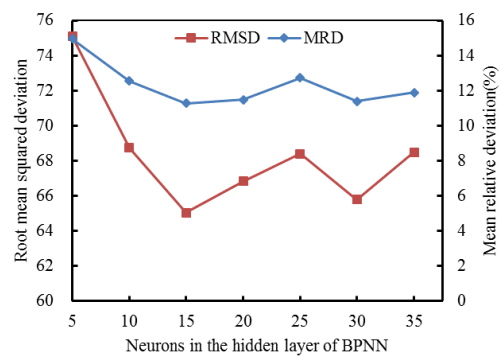
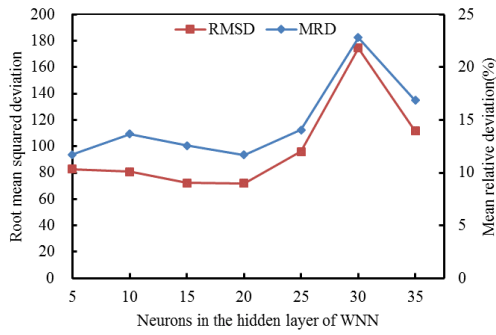


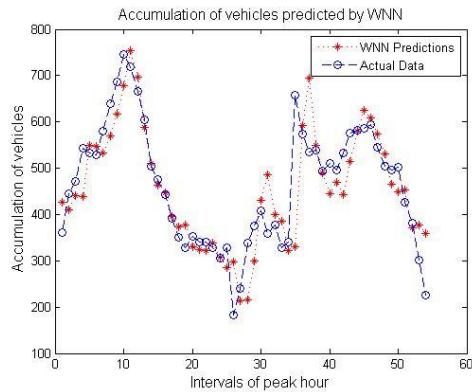
Figure 2: Empirical results of BPNN model: (a) performance comparison among different values of key parameter and (b) prediction results.

### C. Application of WNN

For WNN, the connection weights of the neural network, the expansion parameters and translation parameters of the wavelet function are initialized randomly. Then the initial value of the network learning rate, the error threshold, and maximum iterations are set up. These parameters will be modified by training algorithm. Figure 3(a) shows the RMSE and MRE for each prediction model with respect to the variations of key parameters. As shown in Figure 3(b), when the number of neurons in the hidden layer is around 20, the performance of model achieves best.



(a)

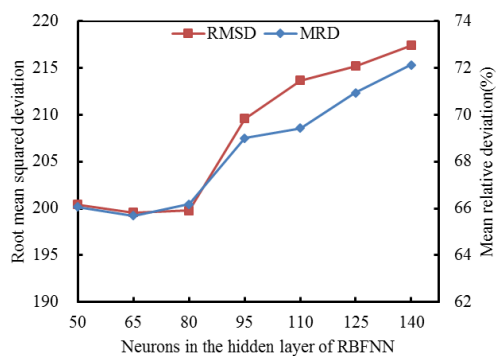


(b)

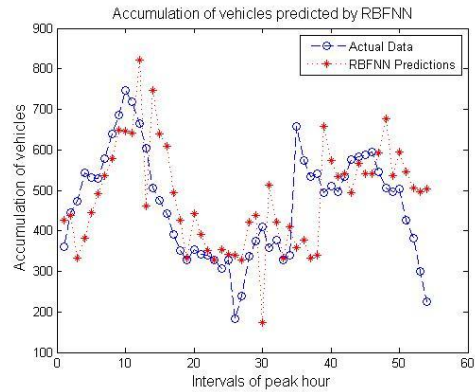
Figure 3: Empirical results of WNN model: (a)performance comparison among different values of key parameter and (b) prediction results.

D. Application of RBFNN

For RBFNN, prediction model is constructed via selection of the centers, the width, and the weights involved in the training procedure firstly. The default of maximum number of neurons in hidden layer is set to be the number of input vectors. The default of mean squared error goal is 0.001. Figure 4(a) shows the RMSE and MRE for each prediction model with respect to the variations of key parameters. As shown in Figure 4(b), for RBFNN, when the number of neurons in the hidden layer is around 65, the model performs best.



(a)

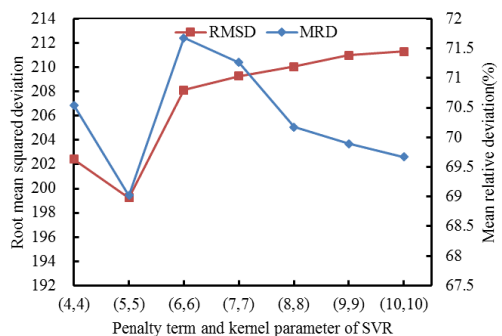


(b)

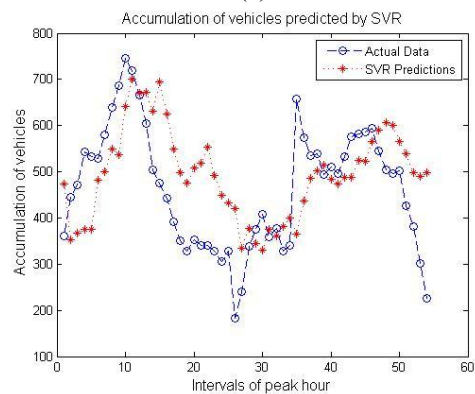
Figure 4: Empirical results of RBFNN model: (a)performance comparison among different values of key parameter and (b) prediction results.

E. Application of SVR

For SVR, training algorithm includes selection of the penalty term  $C$  and the Gaussian kernel parameter  $\gamma$ , which controls SVR quality and strongly affects the performance of the model. Figure 5(a) shows the RMSE and MRE for each prediction model with respect to the variations of key parameters. As shown in Figure 5(b), when the value of penalty term and Gaussian kernel parameter is around (5,5), the performance of model is best.



(a)



(b)

Figure 5: Empirical results of SVR model: (a)performance comparison among different values of key parameter and (b) prediction results.

F. Comparison results

This section compares accumulations dynamical prediction performances of the four short-term forecasting models. Table 1 compares the MAE, the MRE, the MSE, the

RMSE values and computational time of the BPNN, the WNN, the RBFNN, and the SVR.

Table 1: Comparison among four performance indexes (BPNN, WNN, RBFNN and SVR)

	MAE	MRE	MSE	RMSE	Computational Time(seconds)
BPNN	46.14	0.11	4247	65.17	3.81
WNN	48.27	0.12	5190	72.04	9.50
RBFNN	293.54	0.69	44009	209.78	30.89
SVR	285.25	0.71	40978	202.43	9.03

As indicated in Table 1, the maximum MAE value of RBFNN is 293.54, whereas the minimum MAE value of BPNN is as low as 46.14. The MRE value of WNN and BPNN are around 0.11, whereas the MRE value of RBFNN and SVR are almost 0.70. It is shown that the predicting accuracy of the BPNN and the WNN models perform better than other two models. In addition, the RBFNN model costs 30.89 seconds which takes much longer computational time than the other three models. The SVR and WNN models cost about 9 seconds. However, the BPNN model costs only 3.81 seconds. This phenomenon is related to the number of neurons in hidden layer of RBFNN which is larger than other models, which costs much more computational time.

Although the RBFNN and SVR have more robust learning process than the BPNN and WNN, the performance in the study of short-term forecasting of accumulations are not good. This phenomenon illustrates that the less number of neurons in the hidden layer is the crucial point which make models outperform than others. That is because models with less number of neurons in the hidden layer have a larger output feasible area. However, the RBFNN and SVR training function with small input space cannot satisfy the demands of short-term accumulations forecasting. Therefore, much more number of neurons in the hidden layer would be trained to satisfy the larger input space inevitably, which have bad effects on the fitting performance of nonlinear modeling.

To reveal fluctuation variations of the four models, the MRE values of all models throughout the calculation period are computed. As shown in Figure 6(a), the variation range of MRE values of the BPNN model is between -1 and 0.5, and the gap of which is about 1.5. As shown in Figure 6(b), the variation range of MRE values of the WNN model is between -0.7 and 0.6, and the gap of which is less than 1.3. As shown in Figure 6(c), the variation range of MRE values of the RBFNN model is between -1.3 and 0.6, and the gap of which is about 1.9. As shown in Figure 6(d), the variation range of MRE values of the SVR model is between -0.5 and 1.4, and the gap of which is about 1.9. In addition, the MRE values of RBFNN and SVR models have higher values in the beginning and ending of the output dataset. In contrast, the MRE values of the WNN models have the smallest change and slightest fluctuation in the time series that can be observed. Additionally, the fitting effect of the WNN model is best among the four models.

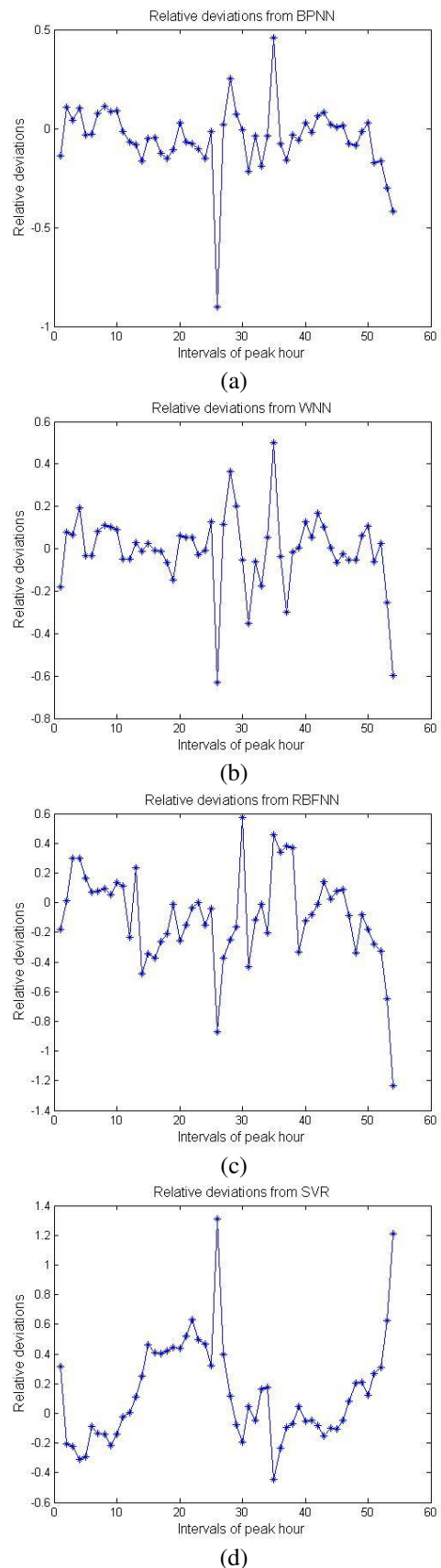


Figure 6: The relative errors from four prediction models.

To summarize, accumulations can be dynamically predicted by the proposed models. However, there are some differences among them in terms of prediction accuracy, stability and computational time. The BPNN and the WNN models have better prediction accuracy and stability than the RBFNN and the SVR models. The WNN and BPNN models are found to be adaptive and have accuracy levels only a sixth

that of RBFNN and SVR models. Additionally, the four models can be improved by intelligent algorithm to make the learning process faster and much more robust.

### VI. CONCLUSION

This paper introduces a new application area of short-term forecasting methods for dynamical prediction of link accumulations, which builds bridges between microscopic traffic flow dynamics and macroscopic system dynamics for traffic monitoring and management. Accumulations has been a main characteristic parameter for expressing traffic state in large urban networks. Accumulations is also the numeric input vectors of short-term accumulations forecasting models. The proposed data-driven approach for accumulation estimation captures traffic accumulations dynamically based on traffic arrivals, departures and network-aggregated demand. The accumulations in the context of MFD are derived from automatic license plate recognition data during rush hour, which gives an accurate calculation of actual accumulations.

Four short-term accumulations forecasting models are tested by comparing their accuracy and efficiency, including BPNN, WNN, RBFNN and SVR. The key parameters of each prediction model are selected by referring to the training performance in case studies. Then the applicability of short-term accumulation forecasting models are compared based on their prediction performances. Comparison results show that the adequacy of WNN and BPNN appear more efficient than that of RBFNN and SVR in the short-term accumulations forecasting problem. Models with less number of neurons in the hidden layer have a larger output feasible area. However, the RBFNN and SVR training functions with small input space are not in line with the expectations of short-term accumulations forecasting problem. The choice of prediction model plays a crucial role in determining forecasting performance. The idealized WNN model with slight fluctuation has better prediction accuracy and stability than other models. In addition, the BPNN model is more feasible than the RBFNN and the SVR models in short-term accumulations forecasting problem.

These findings based on multiple processes provide diverse perspectives to explore alternative solutions for short-term accumulations forecasting problem. The comparative case study gives strong dependence of the choice of prediction methods in the context of MFD-based control schemes.

In the future, researches in this direction would continue with cross-comparing different responsive algorithms and prediction methods in the context of accumulation-based perimeter control schemes. Meanwhile, the selection of suitable forecasting time interval should be aggregated in proper resolution. Moreover, the results of short-term accumulations forecasting models can be used to deal with accumulation-based strategies, such as the optimal perimeter control based on real-time monitoring and traffic flow route guidance for evading saturated road sections. The empirical results in this paper can be extended to predict network-wide accumulations and macroscopic system dynamics.

The short-term accumulations forecasting problem can be

extrapolated to accumulations of subnetworks or large urban network. Modeling the dynamics of macroscopic system and developing real-time perimeter control schemes with accumulation-based strategies seem to be worthwhile. Moreover, the proposed methodology is expected to contribute to traffic flow control in the context of MFD with an unstable congestion state (usually during the rush hours). Optimal control strategies based on pattern recognition could also be developed to prevent the development of over-saturated states of traffic network.

### ACKNOWLEDGMENT

This research has been supported in part by the National Natural Science Foundation of China (Grant 71473060) and National Science and Technology Support Program (Grant 2014BAL05B06). The research has also received funding from the Shenzhen Science and Technology Innovation Commission under agreement (Grant GRCK2015092816025740) and Humanities and social science project of Ministry of Education (Grant 16YJE630003). The authors declare that there is no conflict of interest regarding the publication of this article.

### REFERENCES

- [1] Daganzo, C. F., 2007. Urban gridlock: Macroscopic modeling and mitigation approaches. *Transp. Res. Part B Methodol.* 41 (1), 49–62.  
URL: <https://doi.org/10.1016/j.trb.2006.09.001>
- [2] Geroliminis, N., Daganzo, C. F., 2008. Existence of urban-scale Macroscopic Fundamental Diagrams: Some experimental findings. *Transp. Res. Part B Methodol.* 42 (9), 759–770.  
URL: <https://doi.org/10.1016/j.trb.2008.02.002>
- [3] Smith, B. L., Demetsky, M. J., 1997. Traffic flow forecasting: Comparison of modeling approaches. *J. Transp. Eng.* 123 (4), 261–266.  
URL: [http://dx.doi.org/10.1061/\(asce\)0733-947x\(1997\)123:4\(261\)](http://dx.doi.org/10.1061/(asce)0733-947x(1997)123:4(261))
- [4] Williams, B. M., Hoel, L. A., 2003. Modeling and forecasting vehicular traffic flow as a seasonal ARIMA process: Theoretical basis and empirical results. *J. Transp. Eng.* 129 (6), 664–672.  
URL: [http://dx.doi.org/10.1061/\(asce\)0733-947x\(2003\)129:6\(664\)](http://dx.doi.org/10.1061/(asce)0733-947x(2003)129:6(664))
- [5] Gentile, G., Meschini, L., Papola, N., 2007. Spillback congestion in dynamic traffic assignment: A macroscopic flow model with time-varying bottlenecks. *Transp. Res. Part B Methodol.* 41 (10), 1114–1138.  
URL: <https://doi.org/10.1016/j.trb.2007.04.011>
- [6] Liu, Y., Chang, G. L., 2011. An arterial signal optimization model for intersections experiencing queue spillback and lane blockage. *Transp. Res. Part C Emerg. Technol.* 19 (1), 130–144.  
URL: <https://doi.org/10.1016/j.trc.2010.04.005>
- [7] Lu, Y., Haghani, A., Qiao, W., 2013. Macroscopic traffic flow model for estimation of real-time traffic state along signalized arterial corridor. *Transp. Res. Rec. J. Transp. Res. Board* 2391, 142–153.  
URL: <http://dx.doi.org/10.3141/2391-14>
- [8] Yuan, Y., Lint, H. V., Wageningen-Kessels, F. V., Hoogendoorn, S., 2014. Network-wide traffic state estimation using loop detector and floating car data. *J. Intell. Transp. Syst.* 18 (1), 41–50.  
URL: <http://dx.doi.org/10.1080/15472450.2013.773225>
- [9] Geroliminis, N., Skabardonis, A., 2011. Identification and analysis of queue spillovers in city street networks. *IEEE Trans. Intell. Transp. Syst.* 12 (4), 1107–1115.  
URL: <https://doi.org/10.1109/tits.2011.2141991>
- [10] Ramezani, M., Haddad, J., Geroliminis, N., 2015. Dynamics of heterogeneity in urban networks: Aggregated traffic modeling and hierarchical control. *Transp. Res. Part B Methodol.* 74 (January 2014), 1–19.  
URL: <http://dx.doi.org/10.1016/j.trb.2014.12.010>
- [11] Geroliminis, N., Haddad, J., Ramezani, M., 2013. Optimal perimeter control for two urban regions with Macroscopic Fundamental Diagrams: A model predictive approach. *IEEE Trans. Intell. Transp. Syst.* 14 (1), 348–359.  
URL: <https://doi.org/10.1109/tits.2012.2216877>
- [12] Du, J., Rakha, H., Gayah, V. V., 2016. Deriving macroscopic fundamental diagrams from probe data: Issues and proposed solutions. *Transp. Res. Part C Emerg. Technol.* 66, 136–149.



- URL: <https://doi.org/10.1016/j.trc.2015.08.015>
- [13] Mazloumian, A., Geroliminis, N., Helbing, D., 2010. The spatial variability of vehicle densities as determinant of urban network capacity. *Philos. Trans. R. Soc. A Math. Phys. Eng. Sci.* 368 (1928), 4627–4647.  
URL: <http://dx.doi.org/10.1098/rsta.2010.0099>
- [14] Knoop, V. L., van Lint, H., Hoogendoorn, S. P., 2015. Traffic dynamics: Its impact on the Macroscopic Fundamental Diagram. *Phys. A Stat. Mech. its Appl.* 438, 236–250.  
URL: <http://www.sciencedirect.com/science/article/pii/S0378437115005695>
- [15] Aboudolas, K., Geroliminis, N., 2013. Perimeter and boundary flow control in multi-reservoir heterogeneous networks. *Transp. Res. Part B Methodol.* 55, 265–281.  
URL: <http://dx.doi.org/10.1016/j.trb.2013.07.003>
- [16] van Lint, J. W., 2006. Reliable real-time framework for short-term freeway travel time prediction. *J. Transp. Eng.* 132 (12), 921–932.  
URL: [http://dx.doi.org/10.1061/\(asce\)0733-947x\(2006\)132:12\(921\)](http://dx.doi.org/10.1061/(asce)0733-947x(2006)132:12(921))
- [17] Vlahogianni, E. I., Karlaftis, M. G., Golias, J. C., 2014. Short-term traffic forecasting: Where we are and where we're going. *Transp. Res. Part C Emerg. Technol.* 43, 3–19.  
URL: <http://dx.doi.org/10.1016/j.trc.2014.01.005>
- [18] Dougherty, M. S., Cobbett, M. R., 1997. Short-term inter-urban traffic forecasts using neural networks. *Int. J. Forecast.* 13 (1), 21–31.  
URL: [https://doi.org/10.1016/s0169-2070\(96\)00697-8](https://doi.org/10.1016/s0169-2070(96)00697-8)
- [19] Ou, Y.-K., Liu, Y.-C., Shih, F.-Y., 2013. Risk prediction model for drivers' in-vehicle activities - Application of task analysis and back-propagation neural network. *Transp. Res. Part F Traffic Psychol. Behav.* 18, 83–93.  
URL: <http://dx.doi.org/10.1016/j.trf.2012.12.013>
- [20] Jiang, X., Adeli, H., 2005. Dynamic wavelet neural network model for traffic flow forecasting. *J. Transp. Eng.* 131 (10), 771–779.  
URL: [http://dx.doi.org/10.1061/\(asce\)0733-947x\(2005\)131:10\(771\)](http://dx.doi.org/10.1061/(asce)0733-947x(2005)131:10(771))
- [21] Wu, M., Adeli, H., 2001. Wavelet-neural network model for automatic traffic incident detection. *Math. Comput. Appl.* 6 (3), 85–96.  
URL: <http://dx.doi.org/10.3390/mca6020085>
- [22] Park, J., Sandberg, I. W., 1993. Approximation and Radial-Basis-Function Networks. *Neural Comput.* 5 (2), 305–316.  
URL: <http://www.mitpressjournals.org/doi/abs/10.1162/neco.1993.5.2.305>
- [23] Park, B., Messer, C., II, T. U., 1998. Short-term freeway traffic volume forecasting using radial basis function neural network. *Transp. Res. Rec. J. Transp. Res. Board* 1651, 39–47.  
URL: <http://dx.doi.org/10.3141/1651-06>
- [24] Karim, A., Adeli, H., 2003. Radial basis function neural network for work zone capacity and queue estimation. *J. Transp. Eng.* 129 (5), 494–503.  
URL: [https://doi.org/10.1061/\(asce\)0733-947x\(2003\)129:5\(494\)](https://doi.org/10.1061/(asce)0733-947x(2003)129:5(494))
- [25] Zhu, J. Z., Cao, J. X., Zhu, Y., 2014. Traffic volume forecasting based on radial basis function neural network with the consideration of traffic flows at the adjacent intersections. *Transp. Res. Part C Emerg. Technol.* 47 (P2), 139–154.  
URL: <https://doi.org/10.1016/j.trc.2014.06.011>
- [26] Karim, A., Adeli, H., 2002. Comparison of fuzzy-wavelet radial basis function neural network freeway incident detection model with california algorithm. *J. Transp. Eng.* 128 (1), 21–30.  
URL: [https://doi.org/10.1061/\(asce\)0733-947x\(2002\)128:1\(21\)](https://doi.org/10.1061/(asce)0733-947x(2002)128:1(21))
- [27] Brereton, R. G., Lloyd, G. R., 2010. Support vector machines for classification and regression. *Analyst* 135 (2), 230–267.  
URL: <http://www.ncbi.nlm.nih.gov/pubmed/20098757>
- [28] Castro-Neto, M., Jeong, Y., Jeong, M. K., Han, L. D., 2009. AADT prediction using support vector regression with data-dependent parameters. *Expert Syst. Appl.* 36 (2 PART 2), 2979–2986.  
URL: <https://doi.org/10.2478/v10048-010-0011-9>
- [29] Hu, T.-Y., Ho, W.-M., 2015. Prediction of the impact of typhoons on transportation networks with support vector regression. *J. Transp. Eng.* 141 (4), 4014089.  
URL: [http://dx.doi.org/10.1061/\(asce\)te.1943-5436.0000759](http://dx.doi.org/10.1061/(asce)te.1943-5436.0000759)

**Lei Jin** received the B.S. degree in transportation engineering from Chang'an University, Xi'an, Shannxi, China, in 2012; The M.S. degree in transportation planning and management from Harbin Institute of Technology, Harbin, Heilongjiang, China, in 2014. He is currently working toward the Ph.D. degree in Shenzhen Graduate School, Harbin Institute of Technology. His research interests include road network vulnerability analysis, transportation network optimization and transportation behavior analysis.

**Binglei Xie** received the B.S. degree in applied mathematics from Xinan Jiaotong University, Chengdu, Sichuan, China, in 1996; the M.S. degree in management science and engineering from Xinan Jiaotong University, Chengdu, Sichuan, China, in 1999; the Ph.D. degree in management science and engineering from Xinan Jiaotong University, Chengdu, Sichuan, China, in 2013. He is currently a professor in Shenzhen Graduate School, Harbin Institute of Technology. His research interests include multi-source transportation related data mining, transportation network optimization and transportation behavior analysis.